Allosteric Recognition of Homomeric and Heteromeric Pairs of Monosaccharides by a Foldamer Capsule

Pedro Mateus, Nagula Chandramouli, Cameron Mackereth, Brice Kauffmann, Yann Ferrand, Ivan Huc

Allosteric recognition of homomeric and heteromeric pairs of monosaccharides by a foldamer capsule

Pedro Mateus,[†] Nagula Chandramouli,[†] Cameron D. Mackereth,[‡] Brice Kauffmann,[§] Yann Ferrand,[†,*] Ivan Huc[†,⊥,*]

† Université de Bordeaux, CNRS, Institut Polytechnique Bordeaux, CBMN (UMR 5248), Institut Européen de Chimie et Biologie, 2 Rue Escarpit, 33600 Pessac, France

‡ ARNA (U 1212), Univ. Bordeaux, INSERM, Institut Européen de Chimie et Biologie, 2 rue Robert Escarpit, 33600 Pessac, France

§ Université de Bordeaux, CNRS, INSERM, Institut Européen de Chimie et Biologie (UMS3033/US001), 2 Rue Escarpit, 33600 Pessac, France.

⊥ Department of Pharmacy and Center for Integrated Protein Science, Ludwig-Maximilians-Universität, Butenandstraße 5-13, 81377 Munich – Germany.

KEYWORDS: foldamer, helical capsule, molecular recognition, xylose, arabinose, X-ray crystallography, NMR, circular dichroism.

ABSTRACT: The recognition of either homomeric or heteromeric pairs of pentoses in an aromatic oligoamide double helical foldamer capsule was evidenced by circular dichroism (CD), NMR and X-ray crystallography. The foldamer was obtained readily by combining in a sequence aromatic amino-acids that code both for structural features such as strand curvature and self-assembly properties, together with functional features such as hydrogen bond donors and acceptors. The cavity of the host was predicted to be large enough to accommodate simultaneously two xylose molecules and form a 1:2 complex (one container, two saccharides). Solution and solid state data revealed the selective recognition of the α-$^4C_1$-D-xylopyranose tautomer, which is bound at two identical sites in the foldamer cavity. Circular dichroism titrations demonstrated a positive cooperativity between the first and second binding events. Recognition is diastereoselective, *i.e. P* double helical handedness is quantitatively induced by D xylopyranose. In parallel, we found that the foldamer capsule also binds to arabinose with a 1:1 stoichiometry (one container, one saccharide). A step further was then achieved by sequestrating a heteromeric pair of pentoses, *i.e.* one molecule of α-$^4C_1$-D-xylopyranose and one molecule of β-$^1C_4$-D-arabinopyranose despite the symmetrical nature of the host and despite the similar size of the guests. The 1:1:1 hetero-complex (one container, two different saccharides) was characterized by CD and multidimensional NMR to establish the hydrogen bonding network between the guests and the cavity wall. Subtle and novel induced-fit and allosteric effects are responsible for the outstanding selectivites observed. Altogether, these results further validate helical aromatic amide backbones as a solution of choice to elicit selective carbohydrate recognition.

INTRODUCTION

The development of selective saccharide receptors is a notoriously difficult endeavor, so much so that few research groups dare challenging it.[1] Saccharides nevertheless constitute a central class of biomolecules and their chemical synthesis is an important sub-field of organic chemistry. Discriminating, sensing and selectively manipulating saccharides in water and in organic solvents thus remain subjects of broad interest, and also provide genuine opportunities to push forward the boundaries of molecular recognition. Difficulties to distinguish saccharides stem from the fact that they resemble each other, sometimes differing by a single epimerization, and from the fact that most saccharides exist under more than one α/β anomer or one pyranosyl / furanosyl tautomer. How can one ensure at the same time good binding to one sugar form at the exclusion of all other forms of all other sugars? Synthetic saccharide receptors have been in part inspired by the recognition modes of lectins,[2] the carbohydrate-binding proteins. Obviously, hydrogen-bonding abilities is an advantageous feature to bind a polyhydroxylated guest, but it is not sufficient in polar and protic solvents and in particular in water.[3] The importance of contacts with aromatic rings has been highlighted and exploited,[4-6] as well as coordination to metal ions.[7] Alternatively, boronate ester formation may constitute a strong driving force.[8]

Despite this general knowledge, the *ab initio* design of selective saccharide receptors has not been achieved at the notable exception of receptors for all equatorial sugars which, because of their distinct shape, can be complexed in between two aromatic rings.[5,6] Screening therefore remains a common method. Receptors have been identified from peptide[9] or nucleotide[10] libraries but, even then, success stories are few. A typical approach has consisted in shaping binding sites from first principles and then in screening which sugar binds best. Thus, various families of receptors – macrocycles,[5,6,11] tripods,[12] self-assembled capsules,[13] helically folded containers[7b,14,15] – have been produced which often showed good affinity, and some selectivity, including sometimes for saccharides other than glucose derivatives such as fucose,[6] fructose,[15a] and

mannose.[16] Systematic variations of the receptor structure may then permit improvements of binding selectivity and affinity. A limitation to the rationalization of these improvements has been the scarcity of accurate structural information.

Among the saccharide receptor families mentioned above, helically folded containers with polar inner rims have been developed recently,[15] though their use for simpler guests was established earlier.[17] In the case of aromatic amide helical foldamers, conformations are fully predictable through simple energy minimization, allowing for an accurate design of the cavity volume and positioning of binding features. When the helix has a reduced diameter at both extremities, it can completely surround its guest, i.e. interact with it from all directions and seclude it from the solvent. Guest binding and release then require a local unfolding which slows down these processes.[Erreur ! Signet non défini.7a] Because of their folding mode, such capsules are relatively rigid in all kinds of solvents and therefore operate as size and shape selectors: it was for example possible to bind selectively a dipentose at the exclusion of dihexoses which are too large to fit.[15b] Furthermore, their inherent modular nature – simple oligoamides sequences – provides a quick access to structural variants, using a common synthetic scheme to add, delete, or mutate monomers. Solid phase synthesis may be implemented in the future to give an even quicker access to structural variations,[18] all the more so if it can be automated.

A major advance brought by aromatic-foldamer-based saccharide receptors was straightforward access to detailed structural elucidation, including the very first characterization of complexes *via* single crystal X-ray diffraction at atomic resolution, after twenty five years of research on synthetic saccharide receptors. X-ray data were eventually complemented by NMR validation in solution. Crystal growth was facilitated by the rigid nature of the foldamer helices and by the use of racemic crystallography, through mixing the racemic sugar with the racemic host.[7b,15a,19] Based on this structural information, we showed that it is possible to iteratively design a sugar receptor, *i.e.* to introduce precise modifications so as to enhance selectivity in just a few rounds. Negative design, that is, the preservation of a binding mode to a given guest and the rational introduction of modifications to exclude all other guests was demonstrated.[15a] The rational reversal of guest selectivity was also achieved, using two guests that differ by a single hydroxy group.[17e]

Helical containers thus offer a powerful approach to the design of saccharide recognition, provided a defined structure is available as a starting point. Encouraged by this background, we endeavored to develop a receptor able to bind two monosaccharides simultaneously, a challenge that, to the best of our knowledge, no one has met yet. The study of bi- and multi-molecular recognition has made it possible to explore new forms of stereoisomerism,[20] to perform chemical reactions in confined spaces[21] and to construct supramolecular switches and logic gates.[22] It has been achieved using simpler guests than saccharides and either macrocyclic[23] or self-assembled[24] receptors. Its extension to carbohydrates was initially intended as a curiosity driven molecular recognition challenge and also as a milestone towards receptor mediated selective reactions between unprotected saccharides. As shown in the following, our attempt was successful and also proved to be rich with several important discoveries and lessons. First, the shape and selectivity filter of aromatic amide capsules for saccharide binding is shown to be recurrently effective. Selective binding was not an objective of the current study but an essential result: the few guests that have been tested have a prevailing binding mode with respect to guest conformational / tautomeric / anomeric forms, orientation in the complex, and host handedness, and are thus in principle amenable to structure-based rational iterative improvements. In one case, one complex out of 42 possible host-guest combinations selectively forms. Second, sugar binding in arylamide foldamers is systematicaly optimum when *ca.* 70% of the available space is occupied by the guest. This rule much contrasts with the 55% of space occupancy generally proposed.[25] Third, heteromeric saccharide recognition was found to prevail by simultaneously binding α-$^4C_1$-D-xylopyranose and β-$^1C_4$-D-arabinopyranose, despite the C_2 symmetry of the host, a rather counter-intuitive process. Heteromeric guest binding in symmetrical hosts has been implemented before through space filling:[26] when one guest fills more than half the available space, a second smaller guest is still allowed in the remaining space. But the mechanism here is different and seems to proceed *via* a subtle allostery. Fourth, induced fit and allostery are responsible for the occupation of different binding sites by the same guest depending on whether or not another guest is present. Alternatively, they may prevent the binding of a homomeric pair of a guest that nevertheless can form a heteromeric pair. The intriguing equilibria shown in Figure 1 schematize these findings. Altogether these results validate aromatic oligoamide foldamers as an outstanding platform to quickly advance selective saccharide recognition by synthetic receptors and, quite uniquely, to decipher its complexity. Specifically, their rigid structures that act as size and shape selectors are well adapted to discriminate saccharides, and the small degree of conformational freedom that they nevertheless possess mediates useful allosteric behavior, giving access to sophisticated binding modes.

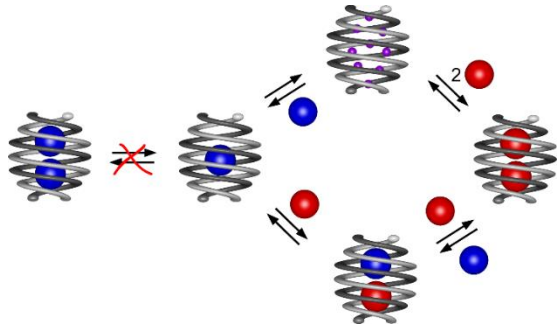

Figure 1. Schematic representation of the reported 1:1 and 1:2 host guest complexes formed from a double helical host and two monosaccharides (red or blue spheres). Top: in the absence of guest, the host is filled by water molecules or solvent (small purple spheres). The blue guest forms a 1:1 complex and cannot form a 1:2 complex alone, but it does in presence of the red guest. Note the blue guest occupies different binding sites in the 1:1 and heteromeric 1:2 complexes.

RESULTS AND DISCUSSION

Design, synthesis and characterization of a double helical capsule. Taking advantage of the predictability of aromatic oligoamide foldamer structures, we previously designed unimolecular capsule **1** (Figure 2D) that proved to be efficient at stereoselectively binding small organic acids.[17a-e] In **1**, the quinoline trimers at each extremity of the strand play the role of

caps closing the helix cavity and also prevent its self-assembly into multiple helices (Figure 2A). Indeed, high helix curvature, as in quinolinecarboxamide oligomers, disfavors the spring-like extension associated with double helix formation.[27] We envisioned that the removal of these trimers would allow the strands to form a stable double helical architecture endowed with a significantly larger cavity compared to a single helical analog (Figure 2B). Oligomer **2** was designed based on this assumption. Its sequence is a modified version of **1** for which the quinoline segments have been replaced by pyridinecarboxamide dimers. The convergent synthesis of **2** involves the coupling of a pivaloyl-PP^{A} mono-acid with the amine of the previously described H_2N-PN_2-BOC triamide[17d] using PyBOP as coupling reagent. After Boc cleavage the amine of pivaloyl-P$_3$N$_2$-NH_2 was coupled twice to the diacid of pyr-pyz-pyr again using PyBOP to provide **2** in moderate yield (see the Supporting Information). In short, the choice of a self-assembled receptor aimed to simplify the synthesis. The different blocks mentioned above can be prepared on multigram scales allowing to readily obtain large amounts (> 1 g.) of sequence **2**.

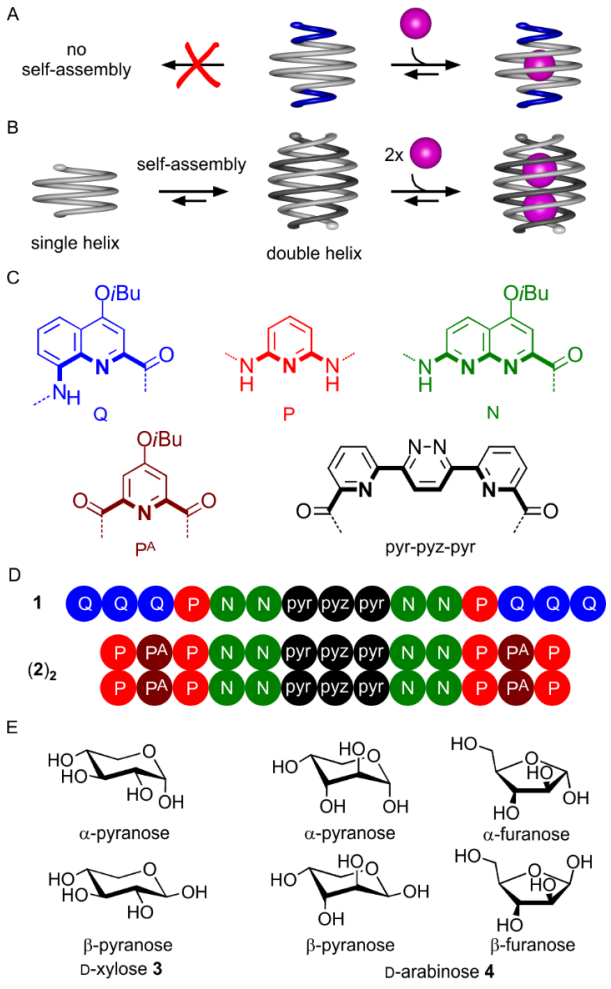

Figure 2. (A) Encapsulation of a guest by a single helical strand possessing a cap (blue) with reduced diameter at both ends preventing dimerization into double helices; (B) single helix – double helix equilibrium (left) and the encapsulation of two guest molecules within the cavity of a duplex. (right); (C) Letter and color codes of the diamine, diacid and amino acid monomers, the bonds shown in bold delineate the inner rim the helix; (D) Oligoamide sequences described in this work. In sequence **1** the two terminal Q units have a terminal 8-nitro group instead of an amino function while in sequence **2** the two terminal P units have a pivaloyl group; (E) Formulae of guest molecules: most abundant tautomeric forms of D-xylose **3**, and D-arabinose **4** in solution.

X-ray-quality single crystals were obtained by slow diffusion of hexane into a chloroform solution of **2**. The solid-state structure was solved and revealed a 2 nm long duplex in which each strand spans three helical turns (Figure 3). The two strands are helically offset with respect to one another by half a turn and extensively stack on top of each other. No other obvious interstrand interactions were noted. The duplex has three pseudo-C_2 symmetry axes, one along the helix axis and two in orthogonal directions.

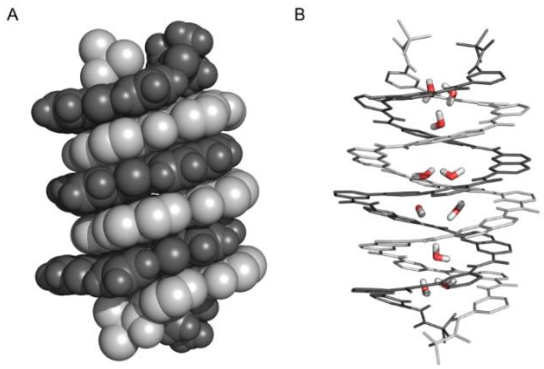

Figure 3. Solid-state structure of (**2**)$_2$: (A) side view shown in CPK representation; (B) side view with 10 encapsulated water molecules. In both representations each strand is colored in a different tone of gray. Side chains have been omitted for clarity.

Evidence of double helix formation was also found in solution. The ^{1}H-NMR spectrum of **2** recorded at 2 mM (Figure S4) shows slightly broadened peaks. The aromatic amide resonances appear in the 10 – 8.5 ppm region, at significantly higher field than is usually found in single helical aryl amide capsules, a hallmark of double helix formation in these systems.[27] Diluting down to 0.05 mM did not allow for the detection of single helix resonances in this solvent. However, the addition of DMSO-d$_6$ (Figure S5), a competitive solvent which disfavors double helix formation, led to the emergence of a second set of sharp signals at lower fields which were assigned to the single helix. In pure DMSO-d$_6$, only the single helix is observed. Indeed, the structure of a crystal grown from DMSO was solved and shown to be the single helix (Figure S22). In $CDCl_3$/DMSO-d$_6$ (9:1 vol/vol) the single helix can be detected as a minor species (at 180 μM). Integration of the signals provided a minimal estimate of the dimerization constant as K_{dim} = 4 10^5 M^{-1}, a value large enough to consider (**2**)$_2$ to be a single entity at the concentrations used in this work.

Prediction of polar guest binding. A trend has emerged from the host-guest properties of various aromatic-amide foldamer capsules studied in independent contexts: tight and selective binding goes along with an occupancy of the host cavity volume by the guest of at least 70%.[17a-f] This rule contrasts with the 55% classically put forward as the optimal value in host guest complexes.[25] A value of 70% is closer to typical packing coefficients in organic solids. The large number and multiple directions of hydrogen bonds between host and guest seem to be the reason for this high space filling. Guests that are smaller

than optimal also bind but with a lower affinity. Guests that are too large for the available space do not bind at all. Another aspect to consider is a weak but non negligeable ability of the host to adjust its conformation to the volume of the guest through slight changes in helix curvature, the pitch remaining constant and equal to the thickness of one aromatic ring. In the few cases where the structure of the host has been elucidated in the absence of guest,[17c,f,28b] *i.e.* when the host is filled with solvent only, the cavity was found to be slightly smaller than in the presence of a guest. For example, **1** has a smaller cavity when it contains one chloroform molecule than when it contains tighly bound tartaric acid.[17f] The folded duplex structure $(\mathbf{2})_2$ has a polar cavity, as evidenced by the presence of 10 crystallographically defined water molecules (Figure 3B), and an inner volume of 280 Å (Figure S23D, E, F). Given the considerations above, we surmised this cavity may be large enough to harbor two aldopentose guests. For instance, xylose has a volume of 107 $Å^3$ and two molecules of xylose would occupy 77% of the cavity volume measured in the absence of guest and, presumably a smaller fraction of the space available in an acutal host-guest complex. In contrast, the volume of a hexose (*ca*. 130 $Å^3$) is clearly too large to fit twice in the cavity of $(\mathbf{2})_2$. We therefore concentrated our efforts to the recognition of pentoses.

Solution and solid state study of D-xylose encapsulation. The ability of $(\mathbf{2})_2$ to bind pentoses was first assessed by titrations in $CHCl_3$/DMSO (9:1 vol/vol) at 298K. A circular dichroism (CD) titration of achiral $(\mathbf{2})_2$ with D-**3** showed the appearance of a negative induced CD signal (Figure 4A) resulting from helix handedness bias. The changes in ellipticity could be fitted to a 1:2 binding model (Figure 4B) which afforded an overall binding constant $K = 2.19\ 10^7\ M^{-2}$ corresponding to K_a values of 69200 M^{-1} and 31600 M^{-1} for the binding of a first and second D-xylose guest, respectively. These values reflect a slight positive cooperativity ($\alpha = 4K_{a2}/K_{a1} = 1.8$), well-illustrated by the sigmoidal binding isotherm (Figure 4C).[29] A ^{1}H-NMR titration under the same conditions revealed the appearance of a single new set of sharp helix signals upon binding of D-**3** (Figure 4D-G). The number of amide resonances (12) is indicative of a pseudo 2-fold symmetry, *i.e.* a lower symmetry than the double helix in the absence of xylose. In agreement with this result was the fact that the ^{1}H-^{13}C HSQC spectrum of the encapsulated uniformly labeled ^{13}C-labelled D-**3** (Figure 4H) recorded in the same conditions shows only one set of correlations suggesting that both bound sugars have the same chemical environment on average. The number of amide signals and the simplicity of the HSQC spectrum also reflect a complete selectivity for a single tautomer of D-**3**, associated to a full diastereoselectivity for a given handedness of the double helix. Based on ^{13}C chemical shift values, on dihedral angle values between CH and OH groups derived from ^3J-coupling constants and on COSY and TOCSY bidimensionnal NMR experiments, it was possible to determine that the two guests are in a α-$^4C_1$-pyranose puckered conformation.

The spontaneous occurrence of such a level of selectivity is significant. Considering the α/β-anomers of the guest and the *P/M*-helicity of the host, six different 1:2 complex may form. Solution data not only show that one of them prevails, but also that one binding mode mode must prevail as well. Despite the many hydrogen bond donors and acceptors on both the guest and host, a particular orientation is preferred.[7b,15] This observation appears to be recurrent with aromatic amide helices, showing their unique capacity to act as size and shape selective filters for complex as complex as saccharides.

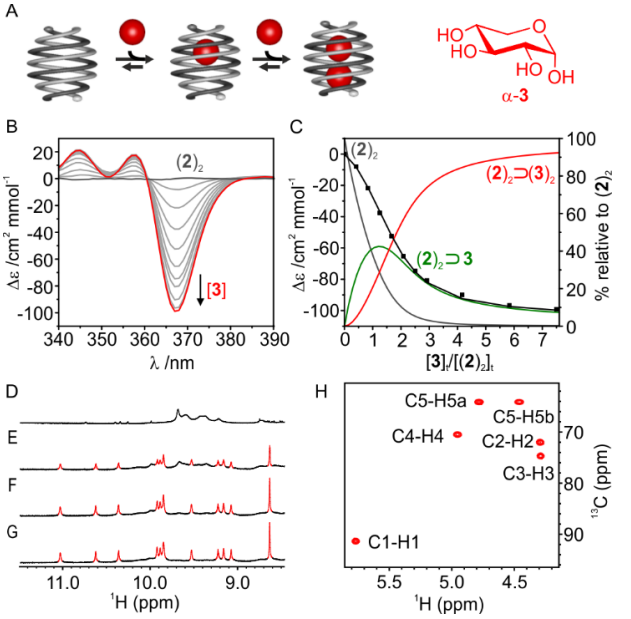

Figure 4. (A) Sequential encapsulation of two guests by a double helical capsule. Red balls represent D-xylose **3**; (B) Induced CD spectra upon binding of D-**3** by $(\mathbf{2})_2$ in $CHCl_3$/DMSO (9:1 vol/vol) at 298K, $[(\mathbf{2})_2]_{tot}$ = 96 µM. The red colored line corresponds to 7.5 equiv. of D-**3** added; (C) Experimental (■) and calculated values (black solid line) for the ICD binding study of receptor $(\mathbf{2})_2$ *vs.* D-**3** with the corresponding species distribution diagram. λ = 367 nm. (D-G) Excerpts from the 400 MHz ^{1}H NMR spectra showing the amide resonances of $(\mathbf{2})_2$ at 1 mM (298K) in $CDCl_3$/DMSO-d_6 (9:1 vol/vol) in the presence of: (D) 0 equiv.; (E) 1 equiv.; (F) 2 equiv. and (G) 3 equiv. of D-**3**. (H) Excerpt of the HSQC spectrum showing ^{1}H-^{13}C correlation signature of two encapsulated uniformly ^{13}C-labelled α-$^4C_1$-D-xylopyranose **3** ($CDCl_3$/DMSO-d_6 9:1 vol/vol).

Further characterization of the complex was performed using 2D and 3D NMR spectroscopy. ^{1}H-^{1}H ROESY recorded at 298K revealed the existence of exchange cross-peaks between protons of the capsule strands reflecting the dynamic nature of the pseudo-C_2 symmetrical complex in solution. The exchange rate between the two populations was measured to be 4.9 ± 0.2 s^{-1}, and thus on the same timescale as the required multidimensional NMR spectra. Decreasing the temperature to 278K suppressed the exchange (Figure S13). This allowed for extensive ^{1}H, ^{13}C and ^{15}N chemical shift assignments of the spectra of $(\mathbf{2})_2 \supset (\text{D-}\mathbf{3})_2$ (Tables S1-3 and Figures S12-13) and the determination of a high-resolution NMR structure of the complex. A final ensemble of 20 structures (Figure 5A) was calculated from distance restraints measured on a sample of ^{13}C-labelled D-**3** bound to ^{13}C-natural abundance $(\mathbf{2})_2$. The use of ^{13}C-edited and -filtered NMR spectra allowed for the collection of 334 unique distance restraints (Figure S12; Table S4), including 82 intermolecular restraints to accurately position the monosaccharides within the capsule cavity and 190 inter- and intra-strand restraints to position the strands relative to one another, as well as the side chains. The structure also revealed the presence of two bound water molecules located at the extremities of the double helix and the assignment of *P* helix handedness. In the complex, the two sugar binding sites are identical and consist of the two inequivalent extremities of the

two strands. The dynamic exchange mentioned above can thus be assigned to a sliding motion of the two strands[30] with respect to one another, along with a concomitant repositioning of each sugar within its cavity.

In parallel, single crystals of the complex were grown by slow diffusion of hexane into a racemic solution of (**2**)$_2$ ⊃ D/L-**3** in $CHCl_3$/chlorobenzene/DMSO (89:10:1 vol/vol/vol), allowing for the elucidation of the solid-state structure by X-ray diffraction analysis (Figure 5C). The use of racemic crystallography recently helped delivering the very first structures of receptor-sugar complexes,[19] but crystal growth is also a consequence of the complex structure being well defined in solution. Overall there is a near perfect superposition of the ensemble of solution structures with the solid-state crystallographic analysis with a r.m.s.d. of 0.054 ± 0.03 Å (Figure S17). As detailed below, the match includes the overall pseudo-C_2 symmetry, the presence and position of the two sugars and the presence of the two water molecules, as well as the *P*-handedness of the double helix containing D-**3**.

The solid-state structure also confirms the α-$^4C_1$-pyranose tautomeric form of the sugars, previously assigned from solution data. The centrosymmetric *P*-1 space group, implies that the crystal lattice also contains two α-$^1C_4$-L-xylopyranose molecules encapsulated by *M*-(**2**)$_2$. The segregation of D- and L-**3** in *P*- and *M*-helices, respectively, is in line with the full diastereoselectivity observed in solution (Figure 4D-H). It is interesting to note that the sugar racemate could also yield a diastereomeric heterocomplex simultaneously including both D-**3** and L-**3**. However, the latter did not crystalize and was not observed either in solution further reflecting high selectivity: the capsule favors homomeric encapsulation of two identical guests in the case of the binding of D-**3** and L-**3**. For example, when a 1:1 (pseudo-racemic) mixture of ^{13}C-labelled D-**3** and ^{13}C-natural abundance L-**3** is added (**2**)$_2$, HSQC spectra confirm that only one type of complex forms.

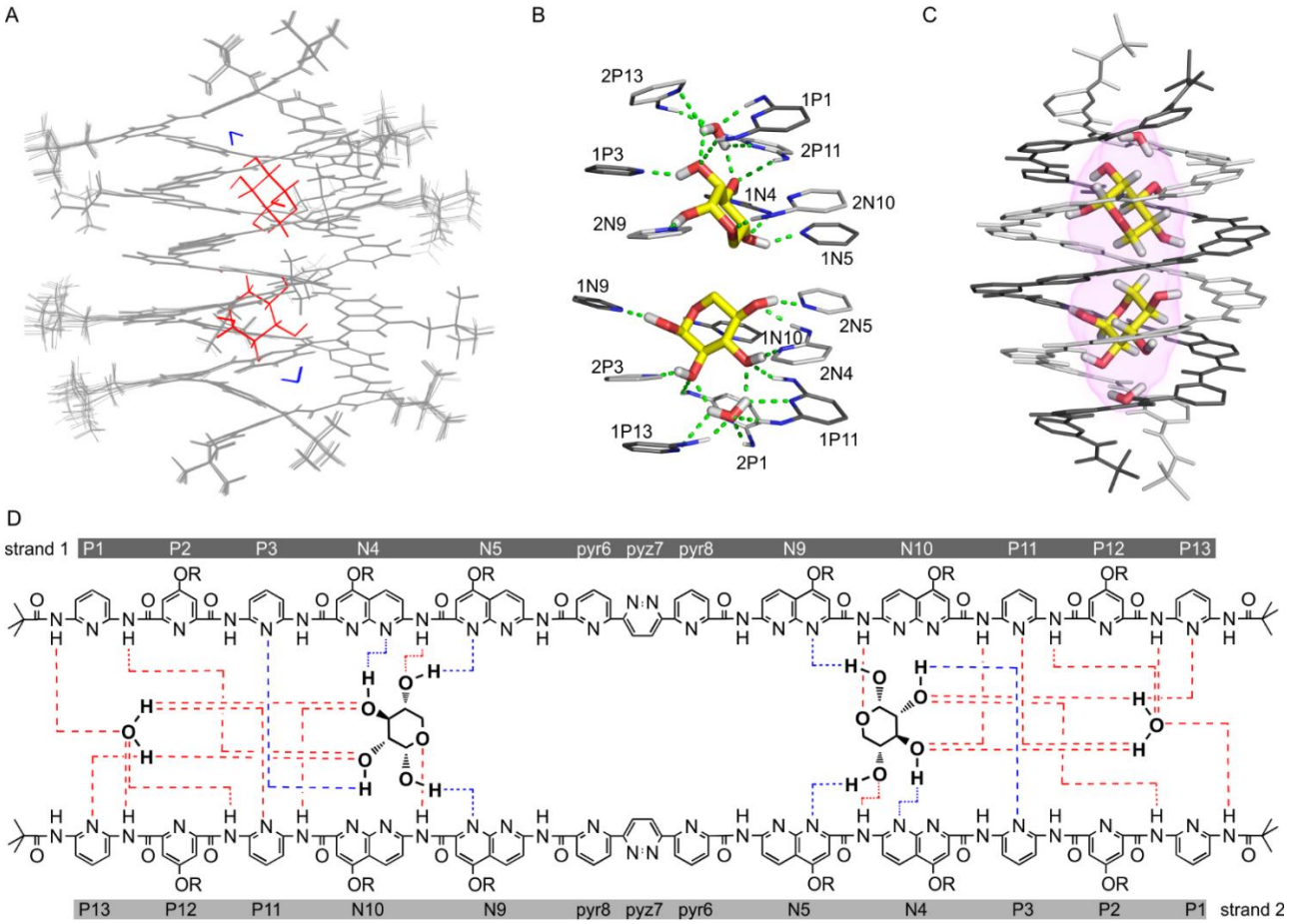

Figure 5. (A) Ensemble of 20 overlaid high-resolution NMR structures of *P*-(**2**)$_2$⊃(α-$^4C_1$-D-xylopyranose)$_2$. The sugars are highlighted in red and the two water molecules in blue; (B) Enlarged side view of the cavity showing the heterocycles that interact with the guests and the water molecules. The heterocycles are color coded in light grey or dark grey depending of the strand they belong to. The 30 hydrogen bonds found in the complex are shown as green dashes. Details of these hydrogen bonds can be found in the supporting information. (C) Solid-state structure of *P*-(**2**)$_2$⊃(α-$^4C_1$-D-xylopyranose)$_2$ shown in tube representation for host and space-filling for the guests. Each strand is colored in a different tone of gray, the two D-**3** guests are colored in yellow. Non-polar hydrogen atoms, isobutoxy side chains and cavity-excluded solvent molecules have been removed for clarity. The volume of the cavity (306 Å^3) is shown as a transparent pink isosurface; (D) Formula and monomer numbering of each strand of the double helical capsule together with the structures of D-**3** represented as Mills projections. Hydrogen bonds where the sugars act as acceptors or donors are shown as red and blue dashed lines, respectively. R stands for isobutyl groups.

In both solution and solid-state structures two water molecules were found encapsulated with the carbohydrates, each occupying an extremity of the cavity. These water molecules are held in position through multiple hydrogen bonds with the amide protons of the terminal pyridine monomer of each strand. Additionally, direct water-to-saccharide hydrogen bonding is observed. As listed in Table S9 and shown in Figure 5B and D, the structures show an extensive array of eight hydrogen bonds between each sugar hydroxyl groups and the inner wall of the helix. As in other foldamer-sugar complexes,[7b-15] no intramolecular hydrogen bonds were found between neighboring hydroxyl groups of the monosaccharides. Instead, only host–guest intermolecular hydrogen bonds occur. Four of the eight hydrogen bonds involve hydroxyl proton donors and the other four involve amide proton donors. Each sugar exposes its endocyclic oxygen atom and methylene group to the center of the cavity, forbidding inter-sugar hydrogen bonds. The weak positive binding cooperativity observed is thus mediated by the helix backbone, not by guest-guest interactions, despite the fact that the guests do not break the symmetry of the host. Comparison of the solid-state structures of the empty host and of the (**2**)$_2$⊃(D-**3**)$_2$ complex confirms that a conformational change takes place upon binding: the two strands of (**2**)$_2$ are helically offset with respect to one another by a quarter of a turn in the complex as opposed to half a turn in the empty capsule, revealing some kind of induced fit at one of the rare degree of structural freedom of the duplex. As a result, the central monomers of each strand are at an angle of about 60° in the complex instead of being in front of each other in the empty capsule. Concomitantly, the inner volume increases from 280 to 306 Å^3 upon guest binding. This allows to calculate that 70% of the volume is occupied by the two xylose molecules, in agreement with the prediction made initially.

Solution studies on D-arabinose binding. The binding of D-arabinose **4**, a pentose that differs from D-**3** by only two stereogenic centers, was then evaluated. A titration of (**1**)$_2$ with D-**4** in $CHCl_3$/DMSO (9:1 vol/vol) at 298K was monitored by CD spectroscopy. A positive signal centered at 370 nm appeared upon increasing the concentration of D-**4** (Figure 6B). CD intensity remained significantly weaker than with D-**3**. In addition, the band at 370 nm had an opposite sign but this did not apply to other bands, hinting at variations of the CD spectra non only through the handedness of the helix but possibly also through the relative positioning of the two strands. In the case of D-**4**, the changes in ellipticity were inconsistent with a 1:2 stoichiometry but instead fitted a 1:1 binding model (Figure 6C) which afforded a K_a value of 21900 M^{-1}, a lower affinity than for D-**3**. A ^{1}H NMR titration in $CDCl_3$/DMSO-d_6 (9:1 vol/vol) at 298K was attempted. However, although spectral changes were clearly visible, the signals were too broad to be interpreted, probably due to guest tumbling and/or the presence of disordered solvent molecules inside the cavity. The same experiment repeated at 243K (Figure 6D-G) revealed the emergence of reasonably sharp amide peaks. As for the CD titration, the spectrum does not change appreciably after addition of 1 equiv. of D-**4**. The same titration was carried out with ^{13}C-labelled D-**4** and monitored by ^{1}H-^{13}C HSQC. Again, addition of more than 1 equiv. of guest did not lead to any variation of the complex resonance pattern (highlighted in blue in Figure 6H-J). The HSQC data revealed two distinct resonances for the anomeric C1 carbon of the ^{13}C-labelled D-**4** encapsulated in (**2**)$_2$. These cross-peaks have a similar ^{13}C chemical shift, and are thus unlikely to correspond to different anomers of the sugar. Instead, we assigned them to diastereoisomeric complexes of a unique anomer of D-**4** being encapsulated either in *P*- or *M*-(**2**)$_2$. Integration of the two cross-peaks allowed calculation of the diastereomeric excess to be 30%, consistent with the lower CD intensity.[31] Based on ^{13}C chemical shift values, on dihedral angle values between CH and OH groups derived from ^3J-coupling constants and on bidimensionnal COSY and TOCSY NMR experiments, it was possible to determine that the guest is in a β-^{1}C$_4$-pyranose puckered conformation. In this conformation only one guest molecule is allowed in the double helix cavity.

The binding of arabinose thus appears to be less selective than for xylose. However, it can be inferred from NMR data that the two complexes observed are well-defined, including the conformation of the sugar. The absence of 1:2 complex even though arabinose is not larger than xylose is also indicative of tight and selective interactions. Arabinose will not migrate to a location of the host cavity that would allow for a second guest to bind. The size and shape selectivity filter of aromatic amide foldamer cavities evoked above is again at play.

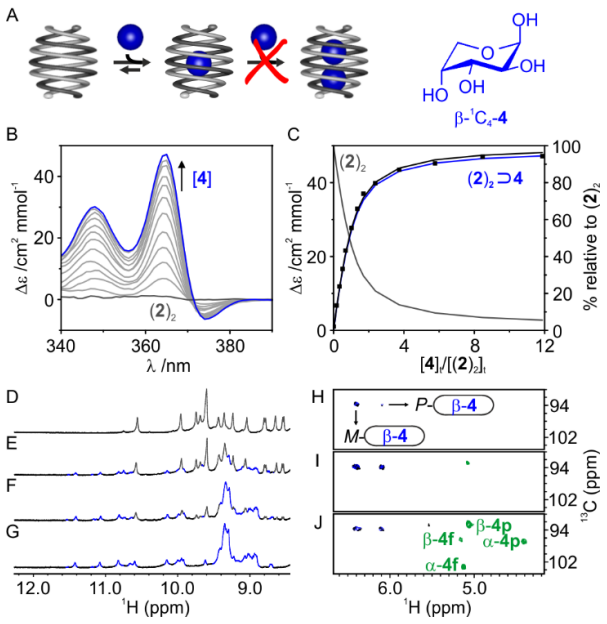

Figure 6. (A) Encapsulation of a single guest by a double helical capsule. Blue balls represent D-arabinose **4**. (B) Induced CD spectra upon binding of D-**4** by (**2**)$_2$ in $CHCl_3$/DMSO (9:1 vol/vol) at 298 K, [(**2**)$_2$] = 120 μM. The blue colored line corresponds to [D-**4**] = 823 μM. (C) Experimental (■) and calculated values (–) for the ICD binding study of receptor (**2**)$_2$ vs. D-**4** with the corresponding species distribution diagram. λ = 365 nm. (D) Excerpts from the 400 MHz ^{1}H NMR spectra showing the amide resonances of capsule (**2**)$_2$ at 1 mM in $CDCl_3$/DMSO-d_6 (9:1 vol/vol) and 243K in the presence of (D) 0 equiv.; (E) 0.5 equiv.; (F) 1.0 equiv. and (G) 2.0 equiv. of D-**4**; Excerpts from ^{1}H-^{13}C HSQC spectra showing the ^{1}H correlations of C1 (anomeric carbon) of uniformly ^{13}C-labelled β-^{1}C$_4$-D-arabinopyranose recorded in the following conditions: (H) [(**2**)$_2$] = 1.0 mM; [D-**4**]= 0.5 mM; (I) [(**2**)$_2$] = 1.0 mM; [D-**4**]= 1.0 mM; (J) [(**2**)$_2$] = 1.0 mM; [D-**4**]= 2.0 mM. Encapsulated and free forms of the sugar are represented in blue and green, respectively. All solutions were prepared in $CDCl_3$/DMSO-d_6 (9:1 vol/vol) and the spectra recorded at 298K.

Structural and thermodynamic study of the formation of a heterodimeric D-xylose-D-arabinose complex. Next, we

sought to evaluate whether a heteromeric pair of pentoses could be encapsulated by $(\mathbf{2})_2$. Monitoring by CD the addition of D-**4** to $(\mathbf{2})_2$ previously equilibrated with excess D-**3** revealed that the initial spectrum, typical of $(\mathbf{2})_2\supset$(D-$\mathbf{3})_2$, changed to eventually reach a final state suggesting some sort of saturation (Figure 7B and C). The final spectrum was very different from that of $(\mathbf{2})_2\supset$(D-**4**), the expected final product if arabinose had simply replaced the two xylose molecules. This result hinted at the possible formation of heteromeric $(\mathbf{2})_2\supset$(D-**3**;D-**4**). The changes in ellipticity could indeed be fitted to such a process (Figure 7C) to afford a K_a value of 46800 M^{-1} for the equilibrium $(\mathbf{2})_2\supset$D-**3** + D-**4** ⇌ $(\mathbf{2})_2\supset$(D-**3**,D-**4**). In other words, D-**4** has an affinity for $(\mathbf{2})_2\supset$D-**3** more than twice as large as for $(\mathbf{2})_2$. Conversely, $(\mathbf{2})_2\supset$D-**3** has a slightly larger affinity for D-**4** than for D-**3**.

Monitoring the same titration by ^{1}H-NMR revealed the emergence of a new set of peaks as D-**4** probably replaces one of the D-**3** guests (Figure 7D-G) to form a heteromeric complex. Consistent with this interpretation, the number of the capsule amide peaks was doubled relative to what was found for the symmetrical $(\mathbf{2})_2\supset$(D-$\mathbf{3})_2$, implying the final structure had no symmetry at all. Titrations with ^{13}C-labelled D-**3** and D-**4** monitored by ^{1}H-^{13}C HSQC eventually provided unequivocal evidence for heterocomplex formation (Figure 7H-J). Upon adding D-**4**, two new cross-peaks appear that correspond to the encapsulated C1 anomeric carbons of both D-**3** and D-**4**. The unambiguous assignment of the sugar resonances was achieved by using ^{13}C-labelled D-**3** in the presence of unlabeled D-**4** and *vice versa* (Figure S9). We also found that increasing the temperature to 318K increased the proportion of the heterocomplex to more than 90% (Figure 7K). This led us to study the effect of temperature for the replacement of D-**3** by D-**4**, which can be described by the equilibrium: $(\mathbf{2})_2\supset$(D-$\mathbf{3})_2$ + D-**4** ⇌ $(\mathbf{2})_2\supset$(D-**3**;D-**4**) + D-**3**. The linear van't Hoff plots (Figure S11) showed that the process is enthalpically disfavored and entropy driven (ΔH=32 kJ mol^{-1}; ΔS=0.11 kJ mol^{-1} K^{-1}, *i.e.* $-T\Delta S$ = –32.8 kJ mol^{-1} at 298 K): below room temperature homocomplex formation is favored while above it heterocomplex formation prevails. The origin of such a large entropic component for a substitution process is unclear and may be related to the release of water molecules as those observed in the absence of sugar (Figure 3). Yet, no such effects have been observed in the other equilibria investigated here or in our earlier studies on foldamer-saccharide recognition.[15]

Detailed structural information could not be gathered using crystallography as single crystals of the hetero-complex could not be obtained. Yet advanced NMR spectroscopy techniques allowed for the structural determination of the complex as shown below. As in the case of $(\mathbf{2})_2\supset$(D-$\mathbf{3})_2$, exchange between the two capsule's strands hampered the resolution of the structure at 298K. Upon cooling down to 278K, the exchange signals disappeared, but the amount of hetero-complex present in solution dropped due to the large entropic term mentioned above. Nevertheless, the concentration of $(\mathbf{2})_2\supset$(D-**3**;D-**4**) remained sufficient for a partial assignment of the resonances (Table S6 and Figs S19,S20). Using combinations of natural abundance and ^{13}C-labelled sugars it was eventually possible to determine an NMR structure of the complex. A final ensemble of 15 structures (Figure 8A) was calculated from a total of 54 distance restraints, including 30 sugar-capsule intermolecular restraints that allowed us to position accurately both pentoses within the capsule cavity, and 24 inter- and intra-sugar restraints to determine the guest's configurations and relative orientation (Figure S18). The structure revealed that the arabinose adopts a β-^{1}C$_4$-D-pyranose conformation whereas the xylose remains in a α-^{4}C$_1$-D-pyranose. As listed in Table S7 and shown in Figure 8B, an array of eight hydrogen bonds between each sugar hydroxyl groups and the inner wall of the helix hold the guests in place. The xylose position is identical to that of the homo-complex. Both pentoses are oriented with their endocyclic oxygen atom pointing to the same side of the cavity leaving OH4 of D-**3** relatively close to OH1 and OH2 of D-**4**.(3.4 Å). Although it was not possible to confidently obtain distance restraints to accurately position the two water molecules located at the extremities of the complex, these

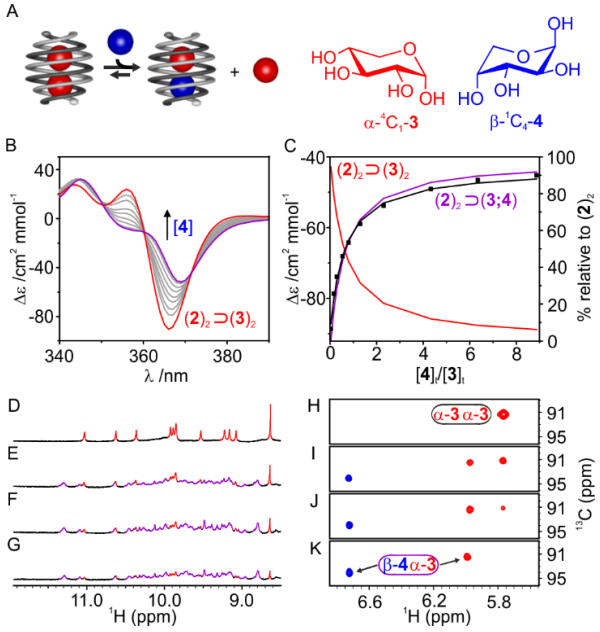

Figure 7. (A) Schematic representation of the replacement of a guest by a different one within a double helical capsule to afford an heterocomplex. D-xylose **3** and D-arabinose **4** are represented in red and blue, respectively; (B) Changes in the CD spectra of $(\mathbf{2})_2\supset$(D-$\mathbf{3})_2$ upon binding of D-**4** in $CHCl_3$/DMSO (9:1 vol/vol) at 298 K. [$(\mathbf{2})_2$] = 94 μM; [D-**3**] = 755 μM. The purple colored line corresponds to [D-**4**] = 4.1 mM; (C) Experimental (■) and calculated values (–) for the ICD binding study of $(\mathbf{2})_2\supset$(D-$\mathbf{3})_2$ vs. D-**4** with the corresponding species distribution diagram. λ = 367 nm. (D) Excerpts from the 400 MHz ^{1}H NMR spectra showing the amide resonances of $(\mathbf{2})_2\supset$(D-$\mathbf{3})_2$ at 1 mM in $CDCl_3$/DMSO-d_6 (9:1 vol/vol) and 298K in the presence of (D) 0 equiv.; (E) 1 equiv.; (F) 2 equiv. and (G) 3 equiv. of D-**4** relative to D-**3**. $(\mathbf{2})_2\supset$(D-$\mathbf{3})_2$ and $(\mathbf{2})_2\supset$(D-**3**,D-**4**) amide resonances are shown in red and purple, respectively. Excerpts from ^{1}H-^{13}C HSQC spectra recorded in $CDCl_3$/DMSO-d_6 (9:1 vol/vol) and 298K showing the ^{1}H correlations of C1 of encapsulated uniformly ^{13}C-labelled α-^{4}C$_1$-D-xylopyranose and β-^{1}C$_4$-D-arabinopyranose recorded in the following conditions: (H) [$(\mathbf{2})_2$] = 1.0 mM; [**3**] = 2.0 mM; previous solution plus (I) [**4**]= 2.0 mM; (J) [**4**] = 6.0 mM. (K) previous solution recorded at, 318K. H1/C1 correlations of D-**3** and D-**4** are represented in red and blue, respectively.

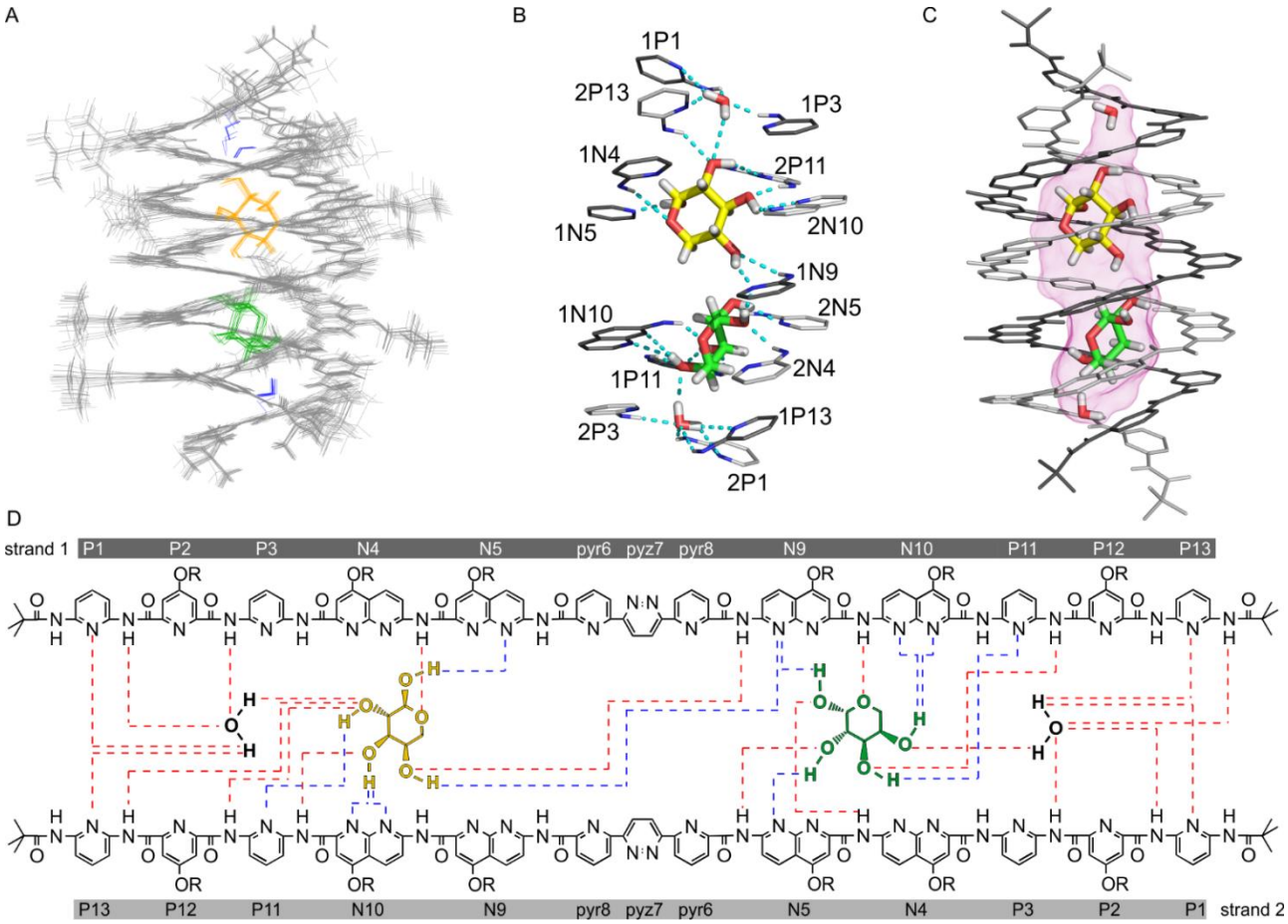

Figure 8. (A) Ensemble of 15 overlaid high-resolution NMR structures of *P*-(**2**)$_2$⊃(α-^{4}C$_1$-D-xylopyranose;β-^{1}C$_4$-D-arabinopyranose). D-**3** and D-**4** are highlighted in yellow and green, respectively; (B) Enlarged side view of the cavity showing the heterocycles that interact with the guests and the water molecules. The heterocycles are color coded in light grey or dark grey depending of the strand they belong to. The hydrogen bonds found in the complex are shown as cyan dashes. Details of these hydrogen bonds can be found in the supporting information. (C) Side view of the complex shown in tube representation for host and space-filling for the guests. Each strand is colored in a different tone of gray. Non-polar hydrogen atoms, isobutoxy side chains and cavity-excluded solvent molecules have been removed for clarity. The volume of the cavity (325 Å^3) is shown as a transparent pink isosurface; (D) Formula and monomer numbering of each strand of the double helical capsule together with the structures of D-**3** and D-**4** represented as Mills projections. Hydrogen bonds where the sugars act as acceptors or donors are shown as red and blue dashed lines, respectively. R stands for isobutyl groups.

were kept in the structure. At last, the inner volume of the cavity was found to be 325 Å^3, a volume slightly larger than the one found for the homo-complex. It thus appears that the replacement of one D-**3** guest by one D-**4** can be mediated by subtle allosteric variations of the structure, but that the changes are important enough for a second substitution not to occur ((**2**)$_2$⊃(D-**4**)$_2$ was not observed). The host-mediated allosteric communication between two guests of identical size and which differ by a single sterogenic center, xylose and arabinose, without contact between them appears to be unique. Usually, a host meant to bind two different guests would be designed with two different binding sites, e.g. to bind an ion pair.[32] Alternatively, symmetrical hosts have been shown to bind to heteromeric pairs of guests when the first guest occupies more than half of the space available, leaving room only to a smaller guest.[25]

As a last set of experiments, we challenged the stereoselectivity of the complexation of both **3** and **4** by (**2**)$_2$ to draw a parallel with the mutual exclusion of D-**3** and L-**3** mentionned above. Thus, the addition of D-**3** to (**2**)$_2$⊃(D-**4**) first produced (**2**)$_2$⊃(D-**3**;D-**4**) and then, with a large excess of D-**3**, led to (**2**)$_2$⊃(D-**3**)$_2$. In contrast, the addition of L-**3** to (**2**)$_2$⊃(D-**4**) does not produce any heteromeric complex. Instead, D-**4** is replaced by L-**3** to first produce (**2**)$_2$⊃(L-**3**) and then (**2**)$_2$⊃(L-**3**)$_2$ (Figure S10). Mind that these competition experiments also involve some changes in helix handedness since (**2**)$_2$⊃(D-**3**)$_2$ is *P* whereas (**2**)$_2$⊃(L-**3**)$_2$ is *M*-helical.

Assessing the general selectivity of sugar binding through the screening of a large number of different pentoses or hexoses to assess was not the purpose of the present investigation. Yet, selectivity eventually turned out to be our main finding. The theoretical outcome of mixing D-xylose and D-arabinose with a racemic *P/M* capsule is that no less than 42 different host-guest complexes may be produced (Figure S21). The observation of a single heteromeric pair of sugars composed of α-^{4}C$_1$-D-xylopyranose and β-^{1}C$_4$-D-arabinopyranose in the *P*-helical foldamer cavity is thus one more example of the highly selective sugar binding in aromatic foldamer cavity.

CONCLUSION

In conclusion, we have prepared a double helical foldamer container with a large internal cavity using a strategy combining

the folding and the self-assembly of a readily accessible aromatic oligoamide strand. The container stereo-selectively encapsulates a single homochiral pair of one xylose tautomer, α-$^4C_1$-D-xylopyranose. We then demonstrated the fully selective complexation of a heteromeric pair of pentoses. These results show the high occurence of spontaneously selective sugar binding within aromatic amide helices that act as stringent shape and selectivity filters. An outcome of the formation of well defined complexes is the possibility to accurately elucidate their structures and unravel the recognition, induced fit and allosteric mechanism at play. In turn, the obtained host-guest complex structures may constitute new starting points for structure-based iterative design and, eventually, the further improvement (i.e. exclusion of all sugars but one) or even the reversal of guest selectivity.[15a,17e] For this purpose, advanced predictive computational tools would bring a major advantage and their development is highly needed. Our results also open up the possibility to precisely design confined spaces that could alter and control the reactivity of native carbohydrates and behave as molecular flasks.

ASSOCIATED CONTENT

Experimental details for synthetic procedures, spectroscopic data, molecular modelling. Crystallographic information files for **2**, $(\mathbf{2})_2$, $(\mathbf{2})_2 \supset$ (D-**3**)$_2$ (CIF). This material is available free of charge via the Internet at http://pubs.acs.org.

AUTHOR INFORMATION

Corresponding Authors

* y.ferrand@iecb.u-bordeaux.fr
* ivan.huc@cup.lmu.de

Author Contributions

The manuscript was written through contributions of all authors.

Funding Sources

This work was supported by the European Union (H2020-MSCA-IF-2015-707071, postdoctoral fellowship to PM) and by an ANR grant (Project ANR-09-BLAN-0082-01, postdoctoral fellowship to NC).

ACKNOWLEDGMENT

This work has benefited from the facilities and expertise of the Biophysical and Structural Chemistry platform at IECB, CNRS UMS3033, INSERM US001, Bordeaux University, France.

REFERENCES

(1) (a) Francesconi, O.; Roelens S. Biomimetic carbohydrate-binding agents (CBAs): binding affinities and biological activities. *ChemBioChem* **2019**, *20*, 1329. (b) S. Tommasone, F. Allabush, Y. K. Tagger, J. Norman, M. Kopf, J. H. R. Tucker, P. M. Mendes The challenges of glycan recognition with natural and artificial receptors. *Chem. Soc. Rev.* **2019** DOI: 10.1039/C8CS00768C.

(2) (a) Gabius, H. J. Biological information transfer beyond the genetic code: the sugar code. *Naturwissenschaften* **2000**, *87*, 108. (b) García-Hernández, E.; Hernández-Arana, A. Structural bases of lectin-carbohydrate affinities: comparison with protein-folding energetics. *Protein Science* **1999**, *8*, 1075. (c) Lee, Y. C.; Lee, R. T. Carbohydrate-protein interactions: basis of glycobiology. *Acc. Chem. Res.*, **1995**, *28*, 321. (d) Toone, E. J. Structure and energetics of protein-carbohydrate complexes. *Curr. Opin. Struct. Biol.* **1994**, *4*, 719. (e) Quiocho, F. A. Protein-carbohydrate interactions: basic molecular features. *Pure & Appl. Chem.* **1989**, *61*, 1293.

(3) (a) Lemieux, R. U. How water provides the impetus for molecular recognition in aqueous solution. *Acc. Chem. Res.* **1996**, *29*, 373. (b) Klein, E.; Ferrand, Y.; Barwell, N. P.; Davis A. P. Solvent effects in carbohydrate binding by synthetic receptors: implications for the role of water in natural carbohydrate recognition. *Angew. Chem., Int. Ed.* **2008**, *48*, 2693.

(4) (a) Asensio, J. L.; Ardá, A.; Cañada, F. J.; Jiménez-Barbero, J. Carbohydrate–aromatic interactions. *Acc. Chem. Res.* **2013**, *46*, 946. (b) Hudson, K. L.; Bartlett, G. J.; Diehl, R. C.; Agirre, J.; Gallagher, T.; Kiessling, L. L.; Woolfson D. N. Carbohydrate–aromatic interactions in proteins. *J. Am. Chem. Soc.* **2015**, *137*, 15152.

(5) (a) Tromans, R. A.; Carter, T. S.; Chabanne, L.; Crump, M. P.; Li, H.; Matlock, J. V.; Orchard, M. G., Davis, A. P. A biomimetic receptor for glucose. *Nat. Chem.* **2019**, *11*, 52. (b) Mooibroek, T. J., Casas-Solvas, J. M.; Harniman, R. L.; Renney, C. M.; Carter, T. S.; Crump, M. P.; Davis A. P. A threading receptor for polysaccharides. *Nat. Chem.* **2016**, *8*, 69. (c) Ke, C.; Destecroix, H.; Crump, M. P.; Davis A. P. A simple and accessible synthetic lectin for glucose recognition and sensing. *Nat. Chem.* **2012**, *4*, 718. (d) Ferrand, Y.; Crump, M. P.; Davis, A. P. A synthetic lectin analog for biomimetic disaccharide recognition. *Science* **2007**, *318*, 619. (e) Klein, E.; Crump, M. P.; Davis, A. P. Carbohydrate recognition in water by a tricyclic polyamide receptor *Angew. Chem., Int. Ed.* **2005**, *44*, 298.

(6) Francesconi, O.; Martinucci, M.; Badii, L.; Nativi, C.; Roelens, S. A biomimetic synthetic receptor selectively recognising fucose in water. *Chem. Eur. J.* **2018**, *24*, 6828.

(7) (a) Striegler, S.; Dittel, M. A sugar discriminating binuclear copper(II) complex. *J. Am. Chem. Soc.* **2003**, *125*, 11518. (b) Mateus, P.; Wicher, B.; Ferrand, Y.; Huc, I. Carbohydrate binding through first- and second-sphere coordination within aromatic oligoamide metallofoldamers. *Chem. Commun.* **2018**, *54*, 5078.

(8) (a) Sun, X.; Chapin, B. M.; Metola, P.; Collins, B.; Wang, B.; James T. D.; Anslyn E. V. The mechanisms of boronate ester formation and fluorescent turn-on in ortho-aminomethylphenylboronic acids. *Nat. Chem.* **2019**, *11*, 768. (b) Sun, X., James, T. D; Anslyn, E. V. Arresting "loose bolt" internal conversion from −B(OH)2 groups is the mechanism for emission turn-On in ortho-aminomethylphenylboronic acid-based saccharide sensors. *J. Am. Chem. Soc.* **2018**, *140*, 2348. (c) Edwards, N. Y., Sager, T. W., McDevitt, J. T.; Anslyn, E. V. Boronic acid based peptidic receptors for pattern-based saccharide sensing in neutral aqueous media, an application in real-life samples. *J. Am. Chem. Soc.* **2007**, *129*, 13575. (d) James, T. D., Samankumara Sandanayake, K. R. A.; Shinkai, S. Chiral discrimination of monosaccharides using a fluorescent molecular sensor. *Nature* **1995**, *374*, 345.

(9) (a) Pal, A.; Berube, M.; Hall, D. G. Design, synthesis, and screening of a library of peptidyl bis(boroxoles) as oligosaccharide receptors in water: identification of a receptor for the tumor marker TF-antigen disaccharide *Angew. Chem., Int. Ed.* **2010**, *49*, 1492. (b) Rauschenberg, M.; Bandaru, S.; Waller, M. P.; Ravoo, B. J. Peptide-based carbohydrate receptors. *Chem. Eur. J.* **2014**, *20*, 2770. (c) Bitta, J.; Kubik S. Cyclic hexapeptides with free carboxylate groups as new receptors for monosaccharides. *Org. Lett.* **2001**, *3*, 2637.

(10) (a) Yang, Q.; Goldstein, I. J.; Mei, H. Y.; Engelke D. R. DNA ligands that bind tightly and selectively to cellobiose. *Proc. Natl. Acad. Sci. (USA)* **1998**, **95**, 5462. (b) Masud M. M.; Kuwahara, M.; Ozaki, H.; Sawai, H. Sialyllactose-binding modified DNA aptamer bearing additional functionality by SELEX. *Bioorg. Med. Chem.* **2004**, *12*, 1111.

(11) (a) Jang, Y.; Natarajan, R.; Ko, Y. H.; Kim, K. Cucurbit[7]uril: a high-affinity host for encapsulation of amino saccharides and supramolecular stabilization of their α-anomers in water.

Angew. Chem., Int. Ed. **2014**, *53*, 1003. (b) Davis, A. P.; Wareham, R. S. A tricyclic polyamide receptor for carbohydrates in organic media. *Angew. Chem., Int. Ed.* **1998**, 37, 2270. (c) Anderson, S.; Neidlein, U.; Gramlich, V.; Diederich, F. A new family of chiral binaphthyl-derived cyclophane receptors: complexation of pyranosides. *Angew. Chem., Int. Ed.* **1995**, *34*, 1596. (d) Kobayashi, K.; Asakawa, Y.; Kato Y.; Aoyama Y. Complexation of hydrophobic sugars and nucleosides in water with tetrasulfonate derivatives of resorcinol cyclic tetramer having a polyhydroxy aromatic cavity: importance of guest-host CH-π interaction. *J. Am. Chem. Soc.* **1992**, *114*, 10307. (e) Perraud, O.; Martinez, A.; Dutasta J.-P. Exclusive enantioselective recognition of glucopyranosides by inherently chiral hemicryptophanes *Chem. Commun.* **2011**, *47*, 5861.

(12) (a) Geffert, C.; Kuschel, M.; Mazik, M. Molecular recognition of N-acetylneuraminic acid by acyclic pyridinium- and quinolinium-based receptors in aqueous media: recognition through combination of cationic and neutral recognition sites. *J. Org. Chem.* **2013**, *78*, 292. (b) Mazik, M.; Cavga, H.; Jones P. G. Molecular recognition of carbohydrates with artificial receptors: mimicking the binding motifs found in the crystal structures of protein−carbohydrate complexes. *J. Am. Chem. Soc.* **2005**, *127*, 9045. (c) Abe, H.; Aoyagi, Y.; Inouye M. A rigid C_{3v}-symmetrical host for saccharide recognition: 1,3,5-Tris(2-hydroxyaryl)-2,4,6-trimethylbenzenes *Org. Lett.* **2005**, *7*, 59. (d) Nativi, C.; Cacciarini, M.; Francesconi, O.; Moneti G.; Roelens, S. A β-mannoside-selective pyrrolic tripodal receptor. *Org. Lett.* **2007**, *9*, 4685. (e) Schmuck, C.; Schwegmann, M. Recognition of anionic carbohydrates by an artificial receptor in water. *Org. Lett.* **2005**, *7*, 3517.

(13) Yamashina, M.; Akita, M.; Hasegawa, T.; Hayashi, S.; Yoshizawa, M. A polyaromatic nanocapsule as a sucrose receptor in water. *Sci. Adv.* **2017**, *3*, e1701126.

(14) (a) Hou, J.-L.; Shao, X.-B.; Chen, G.-J.; Zhou, Y.-X.; Jiang, X.-K.; Li, Z.-T. Hydrogen bonded oligohydrazide foldamers and their recognition for saccharides. *J. Am. Chem. Soc.* **2004**, *126*, 12386. (b) Li, C.; Wang, G.-T.; Yi, H.-P.; Jiang X.-K.; Li, Z.-T.; Wang, R.-X. Diastereomeric recognition of chiral foldamer receptors for chiral glucoses. *Org. Lett.* **2007**, *9*, 1797. (c) Waki, M.; Abe, H.; Inouye, M. Translation of mutarotation into induced circular dichroism signals through helix inversion of host polymers. *Angew. Chem., Int. Ed.* **2007**, *46*, 3059. (d) Abe, H.; Machiguchi, H.; Matsumoto, S.; Inouye, M. Saccharide recognition-induced transformation of pyridine−pyridone alternate oligomers from self-dimer to helical complex. *J. Org. Chem.* **2008**, *73*, 4650. (e) Hwang, J. Y.; Jeon, H.-G.; Choi, Y. R.; Kim, J.; Kang, P.; Lee, S.; Jeong K.-S. Aromatic hybrid foldamer with a hydrophilic helical cavity capable of encapsulating glucose. *Org. Lett.* **2017**, *19*, 5625.

(15) (a) Chandramouli, N.; Ferrand, Y.; Lautrette, G.; Kauffmann, B.; Mackereth, C. D.; Laguerre, M.; Dubreuil, D.; Huc, I. Iterative design of a helically folded aromatic oligoamide sequence for the selective encapsulation of fructose. *Nat. Chem.* **2015**, *7*, 334. (b) Saha, S.; Kauffmann, B.; Ferrand, Y.; Huc, I. Selective encapsulation of disaccharide xylobiose by an aromatic foldamer helical capsule. *Angew. Chem., Int. Ed.* **2018**, *57*, 13542.

(16) Arda, A.; Venturi, C.; Nativi, C.; Francesconi, O.; Gabrielli, G.; Canada, F. J.; Jimenez-Barbero, J.; Roelens S. A chiral pyrrolic tripodal receptor enantioselectively recognizes β-mannose and β-mannosides. *Chem. Eur. J.* **2010**, *16*, 414.

(17) (a) Ferrand, Y.; Huc I. Designing helical molecular capsules based on folded aromatic amide oligomers. *Acc. Chem. Res.* **2018**, *51*, 970. (b) Garric, J.; Léger, J.-M.; Huc, I. Molecular apple peels. *Angew. Chem., Int. Ed.* **2005**, *44*, 1954. (c) Bao, C.; Kauffmann, B.; Gan, Q.; Srinivas, K.; Jiang, H.; Huc, I. Converting sequences of aromatic amino acid monomers into functional three-dimensional structures: second-generation helical capsules. *Angew. Chem., Int. Ed.* **2008**, *47*, 4153. (d) Ferrand, Y.; Kendhale, A. M.; Kauffmann, B.; Grélard, A.; Marie, C.; Blot, V.; Pipelier, M.; Dubreuil, D.; Huc, I. Diastereoselective encapsulation of tartaric acid by a helical aromatic oligoamide. *J. Am. Chem. Soc.* **2010**, *132*, 7858. (e) Lautrette, G.; Wicher, B.; Kauffmann, B.; Ferrand, Y.; Huc, I. Iterative evolution of an abiotic foldamer sequence for the recognition of guest molecules with atomic precision. *J. Am. Chem. Soc.* **2016**, *138*, 10314. (f) Ferrand, Y.; Chandramouli, N.; Kendhale, A. M.; Aube, C.; Kauffmann, B.; Grélard, A.; Laguerre, M.; Dubreuil, D;. Huc, I. Long-range effects on the capture and release of a chiral guest by a helical molecular capsule. *J. Am. Chem. Soc.* **2012**, *134*, 11282. (g) Mateus, P; Wicher, B.; Ferrand, Y.; Huc, I. Alkali and alkaline earth metal ion binding by a foldamer capsule: selective recognition of magnesium hydrate. *Chem. Commun.* **2017**, *53*, 9300.

(18) (a) Dawson, S.J.; Hu, X.; Claerhout, S.; Huc I. Solid phase synthesis of helically folded aromatic oligoamides. *Meth. Enzym.* **2016**, *580*, 279. (b) Baptiste, B.; Douat-Casassus, C.; Laxmi-Reddy, K.; Godde, F.; Huc I. Solid phase synthesis of aromatic oligoamides: application to helical water-soluble foldamers. *J. Org. Chem.* **2010**, *75*, 7175.

(19) Mandal, P. K.; Kauffmann, B.; Destecroix, H.; Ferrand, Y.; Davis, A. P.; Huc I. Crystal structure of a complex between β-glucopyranose and a macrocyclic receptor with dendritic multicharged water solubilizing chains. *Chem.Commun.* **2016**, *52*, 9355.

(20) (a) Tucci, F. C.; Rudkevich, D. M.; Rebek, J. Jr. Stereochemical relationships between encapsulated molecules. *J. Am. Chem. Soc.* **1999**, *121*, 4928. (b) Shivanyuk, A.; Rebek, J., Jr. Social Isomers in Encapsulation Complexes. *J. Am. Chem. Soc.* **2002**, *124*, 12074. (c) Scarso, A.; Shivanyuk, A.; Rebek, J., Jr. Individual solvent/solute interactions through social isomerism. *J. Am. Chem. Soc.* **2003**, *125*, 13981. (d) Scarso, A.; Shivanyuk, A.; Hayashida, O.; Rebek, J., Jr. Asymmetric environments in encapsulation complexes. *J. Am. Chem. Soc.* **2003**, *125*, 6239. (e) Palmer, L. C.; Zhao, Y-L.; Houk, K. N.; Rebek, J., Jr. Diastereoselection of chiral acids in a cylindrical capsule. *Chem. Commun.* **2005**, 3667.

(21) (a) Chen, J.; Rebek Jr., J. Selectivity in an encapsulated cycloaddition reaction. *Org. Lett.* **2002**, *4*, 327. (b) Yoshizawa, M.; Takeyama, Y.; Okano, T.; Fujita, M. Cavity-directed synthesis within a self-assembled coordination cage: highly selective [2 + 2] cross-photodimerization of olefins. *J. Am. Chem. Soc.* **2003**, *125*, 3243. (c) Yoshizawa, M.; Tamura, M.; Fujita, M. Diels-alder in aqueous molecular hosts: unusual regioselectivity and efficient catalysis. *Science* **2006**, *312*, 251. (d) Nishioka, Y.; Yamaguchi, T.; Yoshizawa, M.; Fujita, M. Unusual [2+4] and [2+2] cycloadditions of arenes in the confined cavity of self-assembled cages. *J. Am. Chem. Soc.* **2007**, *129*, 7000. (e) Hou, J-L.; Ajami, D.; Rebek, J., Jr. Reaction of carboxylic acids and isonitriles in small spaces. *J. Am. Chem. Soc.* **2008**, *130*, 7810. (f) Murase, T.; Horiuchi, S.; Fujita, M. Naphthalene Diels−Alder in a self-assembled molecular flask. *J. Am. Chem. Soc.* **2010**, *132*, 2866.

(22) (a) Yoshizawa, M.; Tamura, M.; Fujita, M. AND/OR bimolecular recognition. *J. Am. Chem. Soc.* **2004**, *126*, 6846. (b) Hwang, I.; Ziganshina, A. Y.; Ko, Y. H.; Yun, G.; Kim, K. A new three-way supramolecular switch based on redox-controlled interconversion of hetero- and homo-guest-pair inclusion inside a host molecule. *Chem. Commun.*, **2009**, 416.

(23) (a) Liu, S.; Zavalij, P. Y.; Isaacs, L. Cucurbit[10]uril. *J. Am. Chem. Soc.* **2005**, *127*, 16798. (b) Kikuchi, Y.; Ono, K.; Johmoto, K.; Uekusa, H.; Iwasawa, N. Inclusion of two different guest molecules within a rationally designed macrocyclic boronic ester in organic solvent. *Chem. Eur. J.* **2014**, *20*, 15737. (c) Kim, H-J.; Heo, J.; Jeon, W. S.; Lee, E.; Kim, J.; Sakamoto, S.; Yamaguchi, K.; Kim, K. Selective inclusion of a hetero-guest pair in a molecular host: formation of stable charge-transfer complexes in cucurbit[8]uril. *Angew. Chemie, Int. Ed.* **2001**, *113*, 1574. (d) Han, T.; Chen, C-F. Formation of ternary complexes between a macrotricyclic host

and hetero-guest pairs: and acid-base controlled selective complexation process. *Org. Lett.* **2007**, *9*, 4207. (e) Asadi, A.; Ajami, D.; Rebek, Jr., J. Covalent capsules: reversible binding in a chiral space. *Chem. Sci.*, **2013**, *4*, 1212.

(24) (a) Heinz, T.; Rudkevich, D. M.; Rebek, J., Jr. Molecular recognition within a self-assembled cylindrical host. *Angew. Chemie, Int. Ed.* **1999**, *38*, 1136. (b) Kusukawa, T.; Fujita, M. "Ship-in-a-bottle" formation of stable hydrophobic dimers of cis-azobenzene and -stilbene derivatives in a self-assembled coordination nanocage. *J. Am. Chem. Soc.* **1999**, *121*, 1397. (c) Ebbing, M. H. K.; Villa, M-J.; Valpuesta, J-M.; Prados, P.; de Mendoza, J. Resorcinarenes with 2-benzimidazolone bridges: self-aggregation, self-assembled dimeric capsules, and guest encapsulation. *Proc. Natl. Aacad. Sci. (USA)* **2002**, *99*, 4962. (d) Shivanyuk, A.; Scarso, A.; Rebek, J., Jr. Coencapsulation of large and small hydrocarbons. *Chem. Commun.* **2003**, 1230. (e) Sarwar, M. G.; Ajami, D.; Theodorakopoulos, G.; Petsalakis, I. D.; Rebek, J. Jr. Amplified halogen bonding in a small space. *J. Am. Chem. Soc.* **2013**, *135*, 13672. (f) Nakabayashi, K.; Kawano, M.; Yoshizawa, M.; Ohkoshi, S-i.; Fujita, M. Cavity-induced spin−spin interaction between organic radicals within a self-assembled coordination cage. *J. Am. Chem. Soc.* **2004**, *126*, 16694. (g) Yoshizawa, M.; Ono, K.; Kumazawa, K.; Kato, T.; Fujita, M. Metal−metal d−d interaction through the discrete stacking of mononuclear M(II) complexes (M = Pt, Pd, and Cu) within an organic-pillared coordination cage. *J. Am. Chem. Soc.* **2005**, *127*, 10800. (h) Haino, T.; Kobayashi, M.; Fukazawa, Y. Guest encapsulation and self-assembly of a cavitand coordination capsule. *Chem. Eur. J.* **2006**, *12*, 3310. (i) Yoshizawa, M.; Tamura, M.; Fujita, M. Chirality enrichment through the heterorecognition of enantiomers in an achiral coordination host. *Angew. Chem., Int. Ed.* **2007**, *46*, 3874. (j) Szumna, A. Chiral encapsulation by directional interactions. *Chem. Eur. J.* **2009**, *15*, 12381. (k) Sawada, T.; Yoshizawa, M.; Sato, S.; Fujita, M. Minimal nucleotide duplex formation in water through enclathration in self-assembled hosts. *Nat. Chem.* **2009**, *1*, 53. (l) Sawada, T.; Fujita, M. A Single Watson−Crick G·C base pair in water: aqueous hydrogen bonds in hydrophobic cavities. *J. Am. Chem. Soc.* **2010**, *132*, 7194. (m) Ajami, D.; Dube, H.; Rebek, J., Jr. Boronic acid hydrogen bonding in encapsulation complexes. *J. Am. Chem. Soc.* **2011**, *133*, 9689.

(25) Mecozzi, S.; Rebek, Jr., J. The 55 % Solution : A formula for molecular recognition in the liquid state *Chem. Eur. J.* **1998**, *4*, 1016.

(26) Heinz, T.; Rudkevich, D. M.; Rebek, J., Jr. Pairwise selection of guests in a cylindrical molecular capsule of nanometre dimensions. *Nature* **1998**, *394*, 764.

(27) Berni, E.; Kauffmann, B.; Bao, C.; Lefeuvre, J.; Bassani, D. M.; Huc, I. Assessing the mechanical properties of a molecular spring *Chem. Eur. J.* **2007**, *13*, 8463.

(28) (a) Bao, C.; Gan, Q.; Kauffmann, B.; Jiang, H.; Huc, I. A self-assembled foldamer capsule: combining single and double helical segments in one aromatic amide sequence. *Chem. Eur. J.* **2009**, *15*, 11530. (b) Chandramouli, N.; Ferrand, Y.; Kauffmann, B.; Huc, I. Citric acid encapsulation by a double helical foldamer in competitive solvents. *Chem. Commun.* **2016**, *52*, 3939. (c) Singleton M. L., Pirotte G., Kauffmann B., Ferrand Y., Huc I. Increasing the size of an aromatic helical foldamer cavity by strand intercalation. *Angew. Chem., Int. Ed.* **2014**, *53*, 13140.

(29) (a) Thordarson, P. Determining association constants from titration experiments in supramolecular chemistry. *Chem. Soc. Rev.* **2011**, *40*, 1305. (b) Hunter, C. A.; Anderson, H. L. What is cooperativity? *Angew. Chem., Int. Ed.* **2009**, *48*, 7488.

(30) (a) Berl, V.; Huc, I.; Khoury, R.; Krische, M. J.; Lehn, J.-M. Interconversion of single and double helices formed from synthetic molecular strands. *Nature* **2000**, *407*, 720–723. (b) Ferrand, Y.; Gan, Q.; Kauffmann, B.; Jiang, H.; Huc, I. Template-induced screw motions within an aromatic amide foldamer double helix. *Angew. Chem., Int. Ed.* **2011**, *50*, 7572.

(31) The diasteromeric excess is calculated here using [P complex] – [M complex]) / ([P complex] + [M complex].

(32) He, Q.; Vargas-Zúñiga, G. I.; Kim S. H.; Kim, S. K.; Sessler J. L. Macrocycles as ion pair receptors. *Chem. Rev.* **2019**, *119*, 9753.

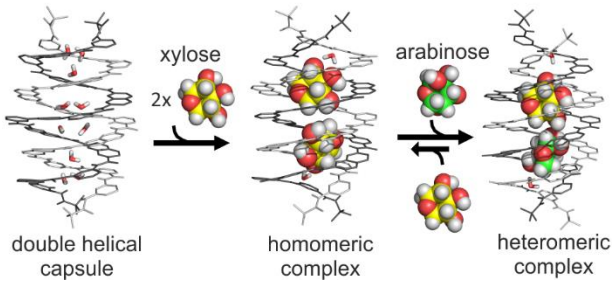
xylose
2x
arabinose
double helical capsule
homomeric complex
heteromeric complex